ORIGINAL PAPER

Hypercapnia Exacerbates the Blood–Brain Barrier Disruption Via Promoting HIF-1a Nuclear Translocation in the Astrocytes of the Hippocampus: Implication in Further Cognitive Impairment in Hypoxemic Adult Rats

Xinqiang Liu[1,2] · Hongguang Ding[2] · Xusheng Li[2] · Yiyu Deng[2] · Xiaoyu Liu[2] · Kangrong Wang[2] · Miaoyun Wen[2] · Shenglong Chen[2] · Wenqiang Jiang[2] · Hongke Zeng[1,2]

Abstract

Hypercapnia in combination with hypoxemia is usually present in severe respiratory disease in the intensive care unit (ICU) and can lead to more severe cognitive dysfunction. Increasing evidence has indicated that the compromised blood–brain barrier (BBB) in the hippocampus in hypoxemia conditions can result in cognitive dysfunction. However, the role and underlying mechanism of hypercapnia in the BBB disruption remains poorly known. A rat model of hypercapnia was first established in this study by intubation and mechanical ventilation with a small-animal ventilator. After this, the cognitive function of the experimental rats was assessed by the Morris water maze test. The BBB permeability was evaluated by the Evans Blue (EB) test and brain water content (BWC). Western blot analysis was carried out to detect the protein expressions of total and nuclear hypoxia-inducible factor-1α (HIF-1α), matrixmetalloproteinase-9 (MMP-9) and Aquaporins-4 (AQP-4) in the hippocampus tissue. Double immunofluorescence further verified the protein expression of different biomarkers was localized in the astrocytes of the hippocampus. Hypercapnia alone did not disrupt the BBB, but it could further enhance the BBB permeability in hypoxemia. Concomitantly, up-regulation of nuclear HIF-1α, AQP-4, MMP-9 protein expression along with increased degradation of the occludin and claudin-5 proteins was found in the hypercapnia rat model, while the total HIF-1α remained unchanged. Interestingly, these changes were independent of the acidosis induced by hypercapnia. Of note, after premedication of 2-Methoxyestradiol (2ME2, an inhibitor of HIF-1α nuclear translocation), the disrupted BBB could be restored resulting in improvement of the cognitive impairment. Meanwhile, accumulation of nuclear HIF-1α, protein expression of AQP-4 and MMP-9 and protein degradation of the occludin and claudin-5 were decreased. Thus, our study demonstrated that hypercapnia can further disrupt the BBB through promoting HIF-1α nuclear translocation and up-regulation of AQP-4 and MMP-9 in hypoxemia. It is therefore suggested that the cascade of hypercapnia-induced nuclear HIF-1α protein translocation in hypoxia-activated astrocytes may be a potential target for ameliorating cognitive impairment.

Keywords Hypercapnia · Blood–brain barrier · Cognitive impairment · Hypoxia-inducible factor-1α · Aquaporins-4 · Matrixmetalloproteinase-9

Xinqiang Liu, Hongguang Ding, and Xusheng Li contributed equally to this work.

✉ Hongke Zeng
  zenghongke@vip.163.com

1   The Second School of Clinical Medicine, Southern Medical University, Guangzhou 510515, Guangdong, People's Republic of China

2   Department of Emergency and Critical Care Medicine, Guangdong Provincial People's Hospital, Guangdong Academy of Medical Sciences, 106 Zhongshan 2nd Road, Guangzhou 510080, Guangdong, People's Republic of China

Introduction

Hypercapnia is usually encountered in some clinical conditions, such as chronic obstructive pulmonary disease (COPD) [1] and acute respiratory distress syndrome (ARDS) [2]. Clinically, the COPD patients had been found to complicate with different degrees of cognitive dysfunction after being discharged [3]. Also, permisssive hypercapnia has been used as a ventilation strategy to reduce the mortality of ARDS [2], but 50% of the ARDS survivors complicate with impaired cognition [4, 5]. Hypoxemia consistently exists in these diseases and has been found to be associated with cognitive dysfunction, but hypercapnia can aggravate the severity [6, 7].

Previous studies have demonstrated that disruption of the blood–brain barrier (BBB) might contribute to the cognitive impairment [8, 9]. Specifically, peripheral inflammation can profoundly impair the central nervous system (CNS) cognition through the compromised BBB [10]. It was well recognized that the most closely related to neurocognition region is in the hippocampal substructure: the CA1 area and the dentate gyrus [11]. Montagne et al. suggested that BBB breakdown in the hippocampus is an early event in the aging human brain that may contribute to cognitive impairment [12]. In light of these findings, it was surmised that hypercapnia can further enhance the BBB permeability which would result in aggravating the cognitive dysfunction in hypoxemia. However, detailed mechanisms involved in hypercapnia-induced BBB disruption in hypoxemia have remained to be elucidated.

Astrocytes play a crucial role in maintaining the integrity and function of the BBB [13]. They are closely related to the BBB permeability through their end-feet which express Aquaporins-4 (AQP-4) [14–17]. In the hypoxic rat model, the BBB is compromised due to the upregulation of AQP-4 expression in the astrocytes [17]. Hypoxemia in combination with hypercapnia can further increase the BBB permeability through up-regulation of AQP-4 expression in the rat model [18]. The tight junction proteins (TJPs) which mainly include claudin, occludin, and zonula protein maintain the BBB normal function. Being the most redox-sensitive part of the TJPs, degradation of the occludin and claudin-5 primarily accounts for the increased BBB permeability in hypoxemia [19, 20]. It is well recognized that the degradation of TJPs is by matrix metalloproteinases (MMPs), of which matrix metalloproteinase-9 (MMP-9) is mainly localized in the astrocytes [21]. In hypoxic newborn pigs during resuscitation, hypercapnia can further induce production of MMPs in the ventricles [22]. Hence, under the condition of hypoxemia, hypercapnia may also promote the production of MMP-9 in the CNS.

Hypoxia-inducible factor-1 (HIF-1) is a heterodimer consisting of the hypoxia-regulated subunit hypoxia-inducible factor-1α (HIF-1α) and the oxygen-insensitive subunit [23]. In hypoxemia, HIF-1α firstly stabilizes in the cytoplasm and then translocates from cytoplasm into the nucleus, where it dimerizes with HIF-1β [24]. The HIF-1 heterodimer binds to hypoxia response elements (HRE), where it modulates the transcription of a host of targets against hypoxic conditions [24]. The previous study has demonstrated that MMP-9 and AQP-4 could be up-regulated by HIF-1α in the CNS [25, 26]. Furthermore, MMP-9 and AQP-4 expression could be further up-regulated by hypercapnia in hypoxemia [18, 22], but the mechanism underpinning this further up-regulation has not been established. As far as we know, oxygen (O_2) consumption is accompanied by carbon dioxide (CO_2) production, hypoxemia and hypercapnia may be perturbed in COPD and ARDS [27, 28]. Hence hypercapnia in combination with hypoxemia may exert different and unique molecular mechanisms unlike that when it acts alone.

In our preliminary study, we have shown that hypercapnia can not increase the expression of HIF-1a total protein in astrocytes of the hippocampus in rats with hypoxemia, but it can further increase the expression of HIF-1a nuclear protein. In light of the above, we hypothesized that hypercapnia may further aggravate the BBB disruption in the adult rats with hypoxemia through the HIF-1 signal pathway. Furthermore, we were interested in searching for the possible drug for ameliorating the hypercapnia-induced neurocognition dysfunction. In this context, we have focused on the drug 2-methoxyestradiol (2ME2), which can confer neuroprotection in the CNS disease [29]. 2ME2 is a naturally occurring derivative of estradiol and devoid of estrogenic activity [30]. It is a potential cancer chemotherapeutic agent, which can tackle cancer with its antiproliferative, proapoptotic, antiangiogenic, anti-tubulin effects [31]. Increasing evidence has shown that the role of 2ME2 on the brain physiology of non-tumor disease is mainly associated with its inhibitory effect on the HIF-1α expression [29].

In the present study, we hypothesized that hypercapnia may further aggravate the BBB disruption in the adult rats with hypoxemia through promoting HIF-1a nuclear translocation. We examined the relationship of hypercapnia, the HIF-1 signal pathway and the HIF-1 target gene (MMP-9 and AQP-4) in the rat model of hypercapnia given 2ME2 pretreatment. We report here that, under the condition of hypoxemia, hypercapnia may promote HIF-1α nuclear translocation and induce over-expression of MMP-9 and AQP-4 in the astrocytes which ultimately would lead to disruption of the BBB integrity.

Material and Methods

Animals and Groups

All animal experiments were conducted under the guidelines for the Care and Use of Laboratory Animals published by the US National Institutes of Health (NIH Publication No. 85-23, revised 2011) and approved by Jinan University Laboratory Animal Ethics Committee (animal approval number: No. 20171011001).

The adult male Sprague Dawley (SD) rats (250–300 g) from the Animal Laboratory of Jinan University were used in this study. Pentobarbital sodium (30 mg/kg) was used to anesthetize the rats through the intraperitoneal injection. After this, the rats were ventilated for 3 h through an animal ventilator (SAR-1000, CWE, Ardmore, PA, USA). The rat model of hypoxemia/hypercapnia that we have previously established [7] suggests that the indicators of blood gas analysis (pH, carbon dioxide partial pressure, and oxygen partial pressure) of SD rats are most stable at 3 h. Therefore, in addition to cognitive impairment, other indicators were acquired at 3 h. The details of the hypoxemic/hypercapnic rat model were described in our previous study [7].

The rats (n = 234, the animal number used in each group was reported in Table 1) were randomly divided into six groups (n = 39 for each): sham-operated group (S group), exposed to the air [7]; hypoxemia group (H group), exposed to 16% O_2 to maintain partial pressure of oxygen (PaO_2) at 55–60 mmHg [7]; hypercapnia group (HC group), exposed to 5% CO_2 to maintain partial pressure of carbon dioxide ($PaCO_2$) at 60–69 mmHg (corresponding pH 7.20–7.25) [7]; hypercapnia hypoxemia group (HH group), HH + 2-Methoxyestradiol (2ME2) group (2ME2 group; 2ME2, an inhibitor of HIF-1α nuclear translocation) and HH + Tris-base group (Tris-base group) (Tris-base was used to buffer the acidosis induced by hypercapnia, but it would not elevate the level of $PaCO_2$), exposed to 5% CO_2 mixing with 16%

O_2 to maintain $PaCO_2$ at 60–69 mmHg (corresponding pH 7.20–7.25) and PO_2 at 55–60 mmHg.

Drug Administration

2ME2 (2ME2, an inhibitor of HIF-1α nuclear translocation, Sigma-AldrichCorp) was dissolved in dimethyl sulfoxide (DMSO) and further diluted in phosphate-buffered saline (PBS) to a final volume of 2 ml (0.125%, 1.25 mg/ml). The inhibitor was administered (5 mg/kg, intraperitoneal injection, the dose–response study of 2ME2 was shown in the Supplemental Document. docx/Supplemental Table. 1, Supplemental Fig. 1) [32]. 1 h before mechanical ventilation in the 2ME2 group. The rats in the S + vehicle group, H + vehicle group, HC group + vehicle group, HH + vehicle group, were injected with an equal volume of DMSO diluted in PBS.

Morris Water Maze (MWM) Test

MWM test was performed to evaluate the murine's memory functions and spatial learning [33]. The apparatus for the test consisted of a round pool (Diameter: 150 cm) filled with warm water (24 ± 2 °C) and a round escape platform (Diameter: 10 cm). The escape platform was fixed in one quadrant and submerged 1 cm under the water surface. One day after the 3 h mechanical ventilation, rats (n = 15 for each group) were allowed to swim for 120 s in the pool to acclimate to the environment and trials. At the second and third day, rats were subjected to the MWM test. The latency time was defined as the time reaching to the platform. Each rat was given 120 s to arrive at the platform and if the rat could not arrive at the platform in 120 s, 120 s was recorded as the latency time. The experimenter guided the rat onto the platform, which was allowed to stay on it for 60 s.

Assessment of (Brain Water Content) BWC

The deeply anesthetized rats (n = 6 for each group) were decapitated after 3 h of mechanical ventilation. The wet weight was obtained immediately by weighing the brain. The dry weight of the brain was obtained after it being heated for 1 day at 100 °C in a drying oven. BWC was calculated as follows: %H_2O = (wet weight − dry weight)/wet weight × 100%.

Evaluation of BBB Integrity

BBB integrity was evaluated by measuring the extravasation of Evans Blue (EB) after 3 h mechanical ventilation. Ten minutes before the end of 3 h ventilation, 2% EB dye (4 ml/kg) was injected intravenously via the tail vein into the rats (n = 6 for each group). In order to remove the excess EB dye in the blood vessels, 110 ml 0.9% saline was used

Table 1 Number of rats sacrificed in different groups

Groups	MWM	BWC	Evans-blue	Western blotting	Immuno-fluorescence
S	15	6	6	6	6
H	15	6	6	6	6
HC	15	6	6	6	6
HH	15	6	6	6	6
2ME2	15	6	6	6	6
Tris-base	15	6	6	6	6

According to the Power (1 − β, 0.80), the Type I error rate (α, 0.05), and the standard deviation (δ) we determined, we calculated the sample size of the rats

to transcardially perfuse the deeply anesthetized rats. After rapid decapitation, the brain was firstly weighed and homogenized in 50% wt/vol trichloroacetic acid, and then centrifuged for 20 min at 10,000 rpm. The supernatants from the brain tissue were collected and analyzed by a spectrophotometer at a wavelength of 620 nm. The total EB content in the brain was quantified in reference to a linear standard curve derived from known amounts of the dye and was expressed as micrograms per gram of tissue.

Western Blotting Analysis

Total or nuclear proteins from the hippocampal tissue (n = 6 for each group) were extracted after 3 h of mechanical ventilation by using a Total Protein Extraction Kit (Nan Jing Key GEN biotechnology, China, Cat. KGP701) or Nuclear Protein Extraction Kit (Bestbio, China; Cat. BB-3102-02) following the manual provided by the manufacturer. The proteins were separated by SDS-polyacrylamide gel electrophoresis and electroblotted to polyvinylidene difluoride (PVDF) membranes. The blots were blocked with 5% nonfat milk for 1 h at room temperature. They were incubated, respectively, with the primary antibodies: HIF-1α (1:1000, Millipore, USA, Cat. MAB5382, RRID: AB_177967), AQP-4 (1:1000, Millipore, USA, Cat. AB3594-50UL, RRID: AB_91530), MMP-9 (1:1000, Millipore, USA, Cat. AB19016, RRID: AB_11211211), HistoneH3 (H3) (1:1000, Abcam, Cambridge, MA, USA, Cat. ab1791, RRID: AB_302613), occludin (1:1000, Abcam, Cambridge, MA, USA, Cat. ab167161, RRID: AB_2756463), claudin-5 (1:1000, Abcam, Abcam, Cambridge, MA, USA, Cat. ab15106, RRID: AB_301652), β-actin (1:1000, Abcam, Cambridge, MA, USA, Cat. ab8226, RRID: AB_306371) and the appropriate horseradish peroxidase-conjugated secondary antibodies at room temperature for 1 h. The secondary antibody was goat anti-rabbit IgG-HRP (1:3000, Cell Signaling Technology, USA, Cat. 7074, RRID: AB_2099233) or goat anti-mouse IgG-HRP (1:3000, Cell Signaling Technology, USA, Cat. 7076, RRID: AB_330924). The membrane was developed using the enhanced chemiluminescence detection system (Millipore, Billerica, MA, USA) and images were developed by an imaging densitometer (ImageQuant LAS 500, GE Healthcare Bio-Sciences AB, Uppsala, Sweden). The relative density was quantified by FluorChem 8900 software (version 4.0.1, Alpha Innotech Corporation, San Leandro, CA, USA). In addition, the expression of target proteins (total HIF-1α, AQP-4, MMP-9, occludin, claudin-5) was normalized to GAPDH as an internal control. H3 was used as an internal control for nuclear HIF-1α protein expression. The specificities of antibodies were demonstrated in the Supplemental Document. docx/ Supplemental Figs. 2–6.

Double Immunofluorescence

Double immunofluorescence was performed to verify HIF-1α, AQP-4 and MMP-9 expression in astrocytes in the CA1 area of the hippocampus (n = 6 for each group). After 3 h mechanical ventilation, the deeply anesthetized rats (n = 6 for each group) were transcardially perfused with ice-cold 0.9% saline rapidly followed by 4% paraformaldehyde. Coronal frozen sections of the removed brain of 10 μm thickness were cut and rinsed in PBS. Four brain sections taken from the hippocampus and four fields of view per slice were randomly taken from each section. Brain sections were blocked and then incubated with the primary antibodies: HIF-1α (1:100, Millipore, USA, Cat. MAB5382, RRID: AB_177967), AQP-4 (1:100, Millipore, USA, Cat. AB3594-50UL, RRID: AB_91530), MMP-9 (1:100, Millipore, USA, Cat. AB19016, RRID: AB_11211211) and GFAP (1:100, Millipore, USA, Cat. MAB360, RRID: AB_11212597) for overnight at 4 °C. On the following day, the brain sections were incubated with fluorescent secondary antibodies: Alexa Fluor® 555 Donkey Anti-Rabbit IgG (H + L) (1:100, Invitrogen Life Technologies, USA, Cat. A31572, RRID: AB_162543), Alexa Fluor® 488 donkey anti-mouse IgG (1:100, Invitrogen Life Technologies, USA; Cat. A21202, RRID: AB_141607) for 1 h at room temperature. Finally, the tissue sections were mounted with a fluorescent mounting medium with DAPI (DAKO Cytomation, Glostrup, Denmark). Cellular co-localization was observed on a confocal microscope (Leica TCS SP2AOBS; Leica Microsystems Ltd., Wetzlar, Germany). Immunohistochemical sections were analyzed under a light microscope (× 100) by Image-Pro Plus 6.0 medical image analysis system. The average HIF1-a/MMP-9/AQP-4 fluorescence density of one single astrocyte in each group was analyzed by the Image-Pro Plus software. The percentage of positive cells in four fields of view per slice was calculated in each group. The specificities of antibodies were demonstrated in the Supplemental Document. docx/Supplemental Figs. 2–6.

Statistical Analysis

The data were analyzed by the software SPSS 20.0. One-way analysis of variance (ANOVA) was carried out to analyze the univariate-factor measurement data and factorial ANOVA for the interaction effects. When an interaction was examined, simple effects analyses were evaluated. Levene test was employed to test the normality and variance homogeneity of the data. Multiple comparisons were analyzed by Fisher's Least Significant Difference test method if the data was homogeneity of variance; otherwise, they were analyzed by Dunnett's T3 method. The difference was considered statistically significant when $p < 0.05$.

Results

Hypercapnia Aggravated Cognitive Dysfunctioninrats with Hypoxemia

Significant interaction effects were observed between hypoxia treatment and hypercapnia treatment at 48 h (df = 1, $F = 7.88$, $p = 0.034$, Fig. 1a), 72 h (df = 1, $F = 8.95$, $p = 0.031$, Fig. 1b), 1 month + 48 h (df = 1, $F = 6.73$, $p = 0.037$, Fig. 1e) and 1 month + 72 h (df = 1, $F = 7.93$,
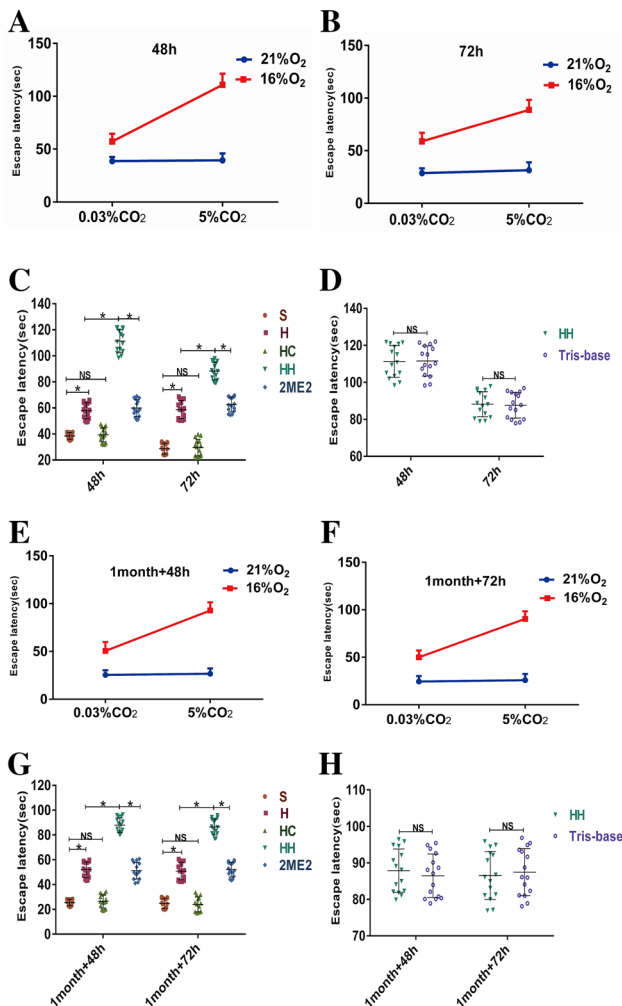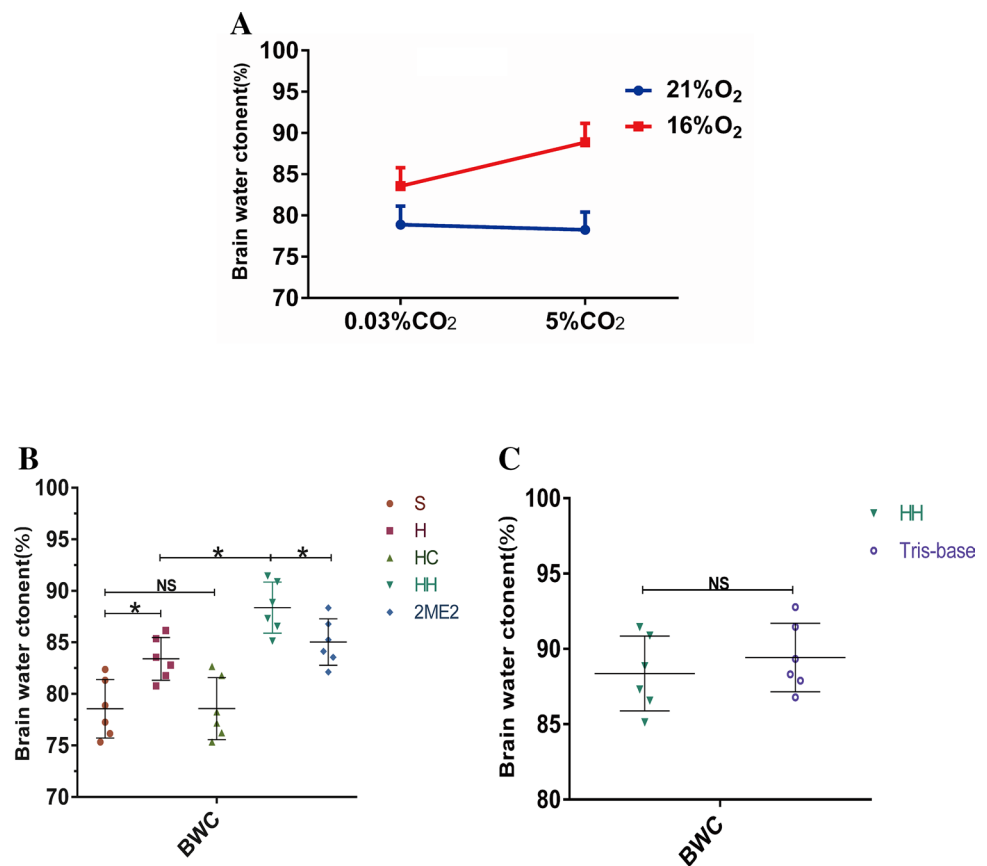

Fig. 1 Significant interaction effects are observed between hypoxia treatment and hypercapnia treatment at 48 h and 72 h (**a** escape latency 48 h; **b** escape latency 72 h; **e** escape latency 1 month + 48 h; **f** escape latency 1 month + 72 h; all *$p < 0.05$). Effects of hypercapnia and 2ME2 on escape latency in each group at 48 h, 72 h, 1 month + 48 h and 1 month + 72 h (**c, g** n = 15). Effects of Tris-base on escape latency in each group at 48 h, 72 h, 1 month + 48 h and 1 month + 72 h (**d, h** n = 15). Each data point refers to a biological replicate (n = 15). Horizontal lines (black) indicate mean ± SD (simple effects analyses). *$p < 0.05$; *NS* non-significant, *$p > 0.05$ (Color figure online)

$p = 0.034$, Fig. 1f). In comparison with S group, a longer escape latency was found in the H group (48 h: df = 1, $F = 11.97$, $p = 0.011$, Fig. 1c; 72 h: df = 1, $F = 41.67$, $p < 0.001$, Fig. 1c; 1 month + 48 h: df = 1, $F = 40.67$, $p < 0.001$, Fig. 1g; 1 month + 72 h: df = 1, $F = 42.33$, $p < 0.001$, Fig. 1g), but not in the HC group (48 h: df = 1, $F = 0.004$, $p = 0.943$, Fig. 1c; 72 h: df = 1, $F = 0.003$, $p = 0.954$, Fig. 1c; 1 month + 48 h: df = 1, $F = 0.002$, $p = 0.967$, Fig. 1g; 1 month + 72 h: df = 1, $F = 0.01$, $p = 0.779$, Fig. 1g). Meanwhile, the longest escape latency was observed in the HH group in comparison with the H group (48 h: df = 1, $F = 41.13$, $p < 0.001$, Fig. 1c; 72 h: df = 1, $F = 19.56$, $p < 0.001$, Fig. 1c; 1 month + 48 h: df = 1, $F = 36.92$, $p < 0.001$, Fig. 1g; 1 month + 72 h: df = 1, $F = 32.98$, $p < 0.001$, Fig. 1g). The escape latency was significantly shortened in rats given 2ME2 (48 h: df = 1, $F = 42.23$, $p < 0.001$, Fig. 1c; 72 h: df = 1, $F = 22.46$, $p < 0.001$, Fig. 1c; 1 month + 48 h: df = 1, $F = 37.87$, $p < 0.001$, Fig. 1g; 1 month + 72 h: df = 1, $F = 33.87$, $p < 0.001$, Fig. 1g). Additionally, when the hypercapnic acidosis was neutralized, no statistically differences were observed between the HH group and Tris-base group (48 h: $p = 0.998$, Fig. 1d; 72 h: $p = 0.999$, Fig. 1d; 1 month + 48 h: $p = 0.997$, Fig. 1h; 1 month + 72 h: $p = 0.996$, Fig. 1h). The individual data of the above each group were shown in the Supplemental Document. docx/Supplemental Table 2.

Hypercapnia Enhanced BWC and BBB Permeability in Rats with Hypoxemia

Significant interaction effects were observed between hypoxia treatment and hypercapnia treatment (BWC: df = 1, $F = 7.54$, $p = 0.033$, Fig. 2a; EB: df = 1, $F = 9.54$, $p = 0.028$, Fig. 3a). Compared with the S group, increased BWC and extravasation of EB were found in the H group (BWC: df = 1, $F = 5.42$, $p = 0.041$, Fig. 2B; EB: df = 1, $F = 75.42$, $p < 0.001$, Fig. 3b), but not in the HC group (BWC: df = 1, $F = 0.001$, $p = 0.992$, Fig. 2b; EB: df = 1, $F = 0.014$, $p = 0.787$, Fig. 3B). Meanwhile, increase in BWC and extravasation of EB was most substantial in the HH group in comparison with H group (BWC: df = 1, $F = 7.12$, $p = 0.034$, Fig. 2b; EB: df = 1, $F = 30.48$, $p < 0.001$, Fig. 3b). Increased BWC and extravasation of EB were significantly reduced by the pretreatmen of 2ME2 (BWC: df = 1, $F = 5.62$, $p = 0.040$, Fig. 2b; EB: df = 1, $F = 21.39$, $p < 0.001$, Fig. 3b). Additionally, when the hypercapnic acidosis was neutralized, no statistically differences were observed between the HH group and Tris-base group (BWC: $p = 0.929$, Fig. 2c; EB: $p = 0.936$, Fig. 3c). The individual data of the above each group were shown in the Supplemental Document. docx/Supplemental Table 3.

Fig. 2 Significant interaction effects are observed between hypoxia treatment and hypercapnia treatment on brain water content (**a** *p* < 0.05). Effects of hypercapnia and 2ME2 on brain water content (**b** n = 6) in each group. Effects of Tris-base on brain water content (**c** n = 6) in each group. Each data point refers to a biological replicate (n = 6). Horizontal lines (black) indicate mean ± SD (simple effects analyses). *p < 0.05; *NS* non-significant, p > 0.05 (Color figure online)

Hypercapnia Augmented the Expression of AQP-4 and MMP-9 and Accumulation of the Nuclear HIF-1α in the Hypoxemic Hippocampus

Significant interaction effects were found between hypoxia treatment and hypercapnia treatment in terms of nuclear HIF-1α (df = 1, $F = 12.44$, $p = 0.008$, Fig. 4d), AQP-4 (df = 1, $F = 22.70$, $p < 0.001$, Fig. 5c) and MMP-9 (df = 1, $F = 19.62$, $p = 0.004$, Fig. 5d) expression, but not for the total HIF-1α expression (df = 1, $F = 0.09$, $p = 0.695$, Fig. 4c). Compared with the S group, increased total HIF-1α protein, nuclear HIF-1α protein, AQP-4 and MMP-9 expression was found in the H group (total HIF-1α/β-actin: df = 1, $F = 122.97$, $p < 0.001$, Fig. 4a, e; nuclear HIF-1α/H3: df = 1, $F = 142.95$, $p < 0.001$, Fig. 4b, e; AQP-4/β-actin: df = 1, $F = 181.29$, $p < 0.001$, Fig. 5a, e; MMP-9/β-actin: df = 1, $F = 196.32$, $p < 0.001$, Fig. 5b, e), but not in the HC group (total HIF-1α/β-actin: df = 1, $F = 0.004$, $p = 0.976$, Fig. 4a, e; nuclear HIF-1α/H3: df = 1, $F = 0.16$, $p = 0.534$, Fig. 4b, e; AQP-4/β-actin: df = 1, $F = 0.015$, $p = 0.768$, Fig. 5a, e; MMP-9/β-actin: df = 1, $F = 0.007$, $p = 0.918$, Fig. 5b, e). Meanwhile, increased protein expression for the markers was most pronounced in the HH group in comparison with the H group (nuclear HIF-1α/H3: df = 1, $F = 118.94$, $p < 0.001$, Fig. 4b, e; AQP-4/β-actin: df = 1, $F = 62.43$, $p < 0.001$, Fig. 5a, e; MMP-9/β-actin:

df = 1, $F = 28.75$, $p < 0.001$, Fig. 5b, e). There was no significant difference between the HH group and H group in the protein expression of total HIF-1α (total HIF-1α/β-actin: df = 1, $F = 0.15$, $p = 0.545$, Fig. 4a, e). Increased AQP-4, MMP-9 and nuclear HIF-1α protein expression was significantly reduced by the pretreatmen of 2ME2 (AQP-4/β-actin: df = 1, $F = 63.73$, $p < 0.001$, Fig. 5a, e; MMP-9/β-actin: df = 1, $F = 31.69$, $p < 0.001$, Fig. 5b, e; nuclear HIF-1α/H3: df = 1, $F = 96.73$, $p < 0.001$, Fig. 4b, e). Additionally, when the hypercapnic acidosis was neutralized, no statistically differences were observed between the HH group and Tris-base group (total HIF-1α/β-actin: $p = 0.898$, Fig. 4a, f; nuclear HIF-1α/H3: $p = 0.916$, Fig. 4b, f; AQP-4/β-actin: $p = 0.873$, Fig. 5a, f; MMP-9/β-actin: $p = 0.938$, Fig. 5b, f). The individual data of the above each group were shown in Supplemental Document. docx/Supplemental Table 4. The full western blots of the above each group were shown in the Supplemental Document. docx/Supplemental Figs. 7–10.

Hypercapnia Decreased the Expresssion Level of Occludin and Claudin-5 Protein in the Hypoxemic Hippocampus

Significant interaction effects were found between hypoxia treatment and hypercapnia treatment in terms of occludin
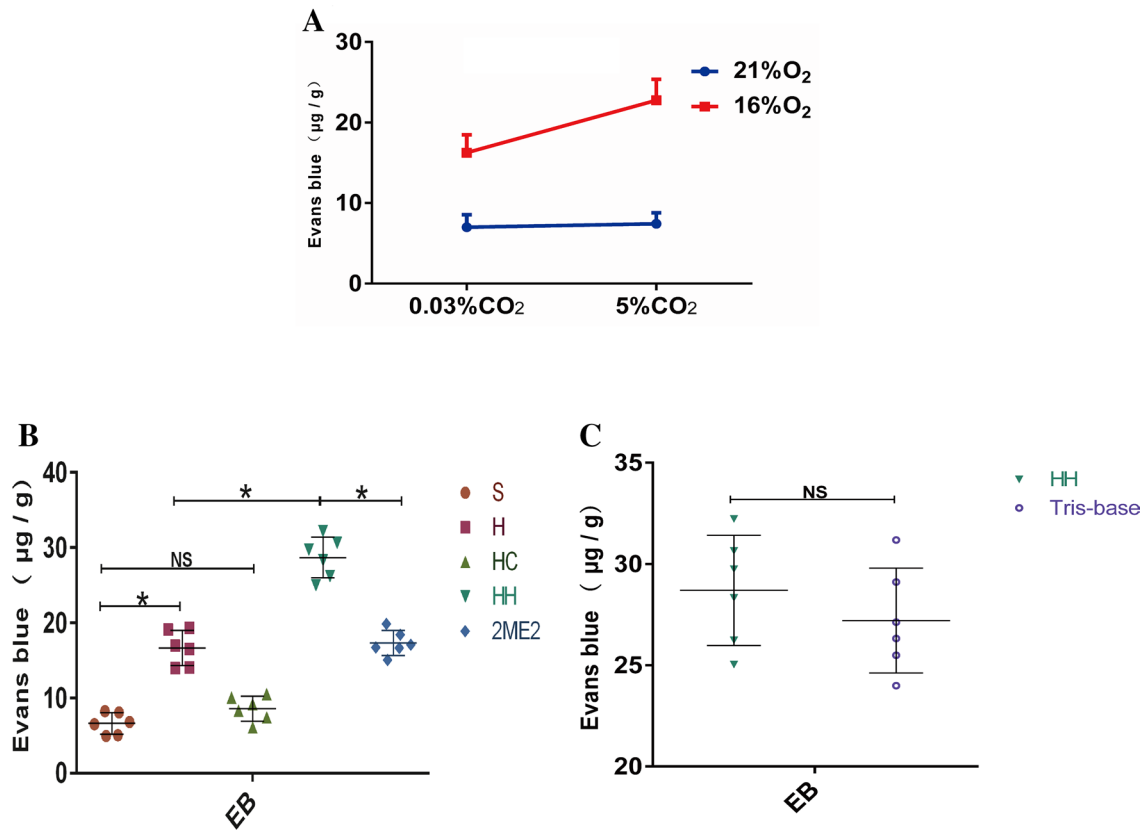
Fig. 3 Significant interaction effects are observed between hypoxia treatment and hypercapnia treatment on Evans Blue (**a** *$p < 0.05$). Effects of hypercapnia and 2ME2 on Evans Blue (**b** n = 6) in each group. Effects of Tris-base on Evans Blue (**c** n = 6) in each group.

Each data point refers to a biological replicate (n = 6). Horizontal lines (black) indicate mean ± SD (simple effects analyses). *$p < 0.05$; *NS* non-significant, $p > 0.05$ (Color figure online)

(df = 1, $F = 27.74$, $p < 0.001$, Fig. 6c) and claudin-5 (df = 1, $F = 36.89$, $p < 0.001$, Fig. 6d) expression. Compared with the S group, decreased occludin and claudin-5 protein expression was found in the H group (occludin/β-actin: df = 1, $F = 47.93$, $p < 0.001$, Fig. 6a, e; claudin-5/β-actin: df = 1, $F = 47.91$, $p < 0.001$, Fig. 6b, e), but not in the HC group (occludin/β-actin: df = 1, $F = 0.021$, $p = 0.497$, Fig. 6a, e; claudin-5/β-actin: df = 1, $F = 0.052$, $p = 0.383$, Fig. 6b, e). Decrease in protein expressions was most drastic in the HH group in comparison with the H group (occludin/β-actin: df = 1, $F = 77.69$, $p < 0.001$, Fig. 6a, e; claudin-5/β-actin: df = 1, $F = 54.89$, $p < 0.001$, Fig. 6b, e). Decrease of protein expression was significantly attenuated by 2ME2 pretreatment (occludin/β-actin: df = 1, $F = 72.71$, $p < 0.001$, Fig. 6a, e; claudin-5/β-actin: df = 1, $F = 66.84$, $p < 0.001$, Fig. 6b, e). Additionally, when the hypercapnic acidosis was neutralized, no statistically differences were observed between the HH group and the Tris-base group (occludin/β-actin: $p = 0.789$, Fig. 6a, f; claudin-5/β-actin: $p = 0.698$, Fig. 6b, f). The individual data of the above each group were shown in Supplemental Document. docx/Supplemental Table 4. The full western blots of the above each group were shown in

the Supplemental Document. docx/Supplemental Figs. 11 and 12.

Hypercapnia Augmented the Expresssion of AQP-4, MMP-9 and Nuclear HIF-1α in the Astrocytes of Hypoxemic Hippocampus

In the HC group, hypercapnia alone did not exert any noticeable effect on the immunofluorescence of AQP-4, MMP-9 and nuclear HIF-1α without hypoxemia (nuclear HIF-1α: no white arrow in Fig. 7a; AQP-4: Fig. 8a, Fluorescence density: df = 1, $F = 0.004$, $p = 0.947$, Fig. 8c and %AQP-4 positive cells: df = 1, $F = 0.003$, $p = 0.956$, Fig. 8e; MMP-9: no white arrow in Fig. 9a). However, in comparison with the S group, the immunofluorescence of all markers was significantly enhanced in the H group (nuclear HIF-1α: white arrow in Fig. 7a; AQP-4: white arrow in Fig. 8a, Fluorescence density: df = 1, $F = 173.23$, $p < 0.001$, Fig. 8c and %AQP-4 positive cells: df = 1, $F = 148.91$, $p < 0.001$, Fig. 8e; MMP-9: white arrow in Fig. 9a). Meanwhile, in comparison with the H group, the immunofluorescence of AQP-4, MMP-9 and nuclear
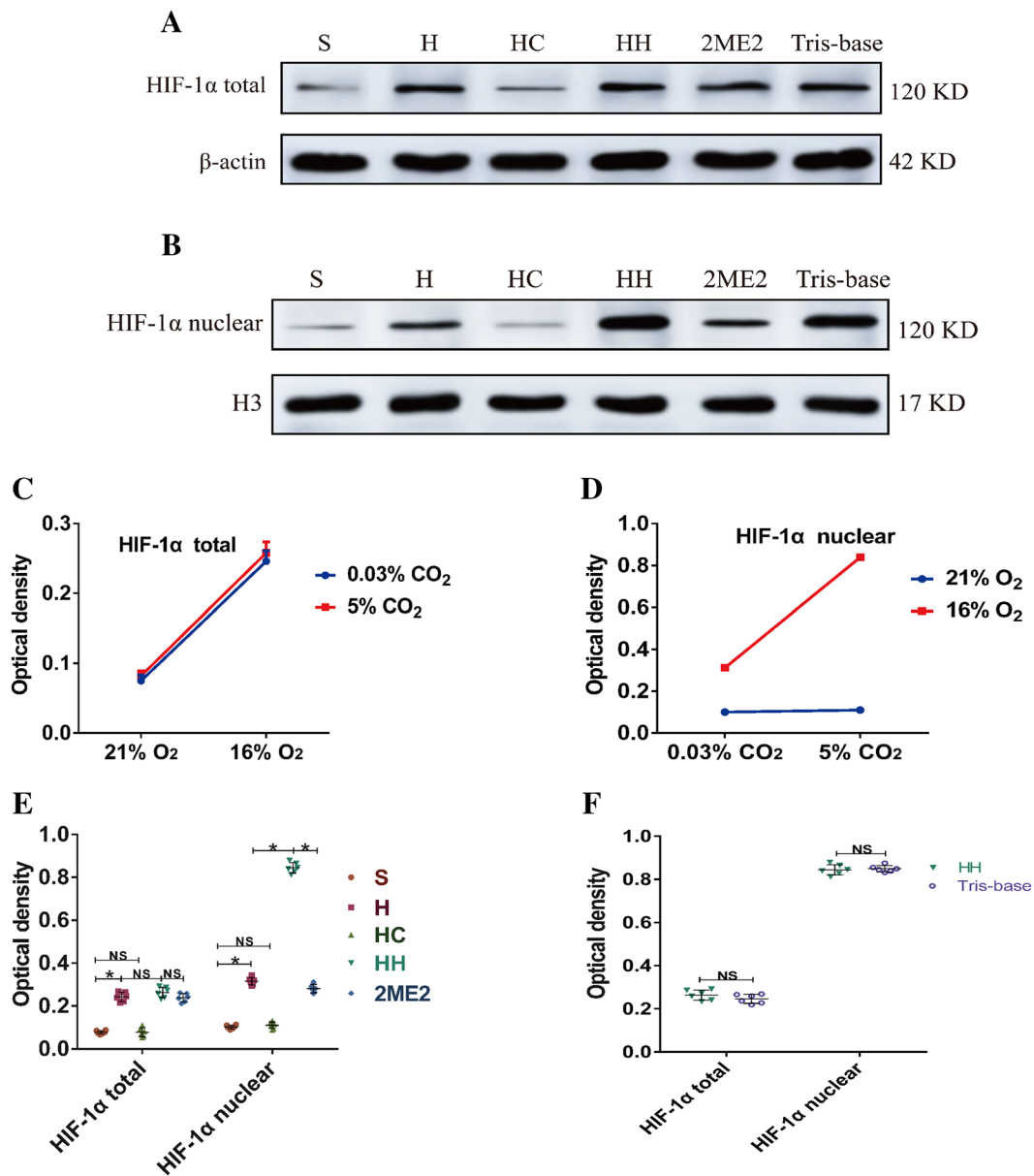
Fig. 4 The immunoreactive bands of total HIF-1α (**a**), β-actin (**a**), nuclear HIF-1α (**b**) and H3 (**b**). β-actin and H3 expression were measured as control; No interaction effect is observed between hypoxia treatment and hypercapnia treatment (**c** total HIF-1α, $p > 0.05$). There are significant interaction effects between hypercapnia treatment and hypoxia treatment (**d** nuclear HIF-1α, *$p < 0.05$). Effects of hypercapnia and 2ME2 on the protein expression levels of total HIF-1α (**e**), nuclear HIF-1α (**e**) in each group (n=6). Effects of Tris-base on the protein expression levels of total HIF-1α (**f**), nuclear HIF-1α (**f**) in each group (n=6). The expression of total HIF-1α and nuclear HIF-1α was normalized with β-actin and H3 protein levels, respectively. Each data point refers to a biological replicate (n=6). Horizontal lines (black) indicate mean ± SD (simple effects analyses). *$p < 0.05$; *NS* non-significant, $p > 0.05$. *HIF-1α* hypoxia-inducible factor-1α (Color figure online)

HIF-1α was further enhanced in the HH group (nuclear HIF-1α: white arrow in Fig. 7a, Fluorescence density: df = 1, F = 63.71, $p < 0.001$, Fig. 7c and %HIF-1α positive cells: df = 1, F = 34.82, $p < 0.001$, Fig. 7e; AQP-4: white arrow in Fig. 8a, Fluorescence density: df = 1, F = 39.43, $p < 0.001$, Fig. 8c and %AQP-4 positive cells: df = 1, F = 38.96, $p < 0.001$, Fig. 8e; MMP-9: white arrow in Fig. 9a, Fluorescence density: df = 1, F = 59.46, $p < 0.001$, Fig. 9c and %MMP-9 positive cells: df = 1, F = 48.99, $p < 0.001$, Fig. 9e). 2ME2 pretreatment attenuated the immunofluorescence of AQP-4, MMP-9 and nuclear HIF-1α (nuclear HIF-1α: white arrow in Fig. 7a, Fluorescence density: df = 1, F = 51.21, $p < 0.001$, Fig. 7c and %HIF-1α positive cells: df = 1, F = 18.95,
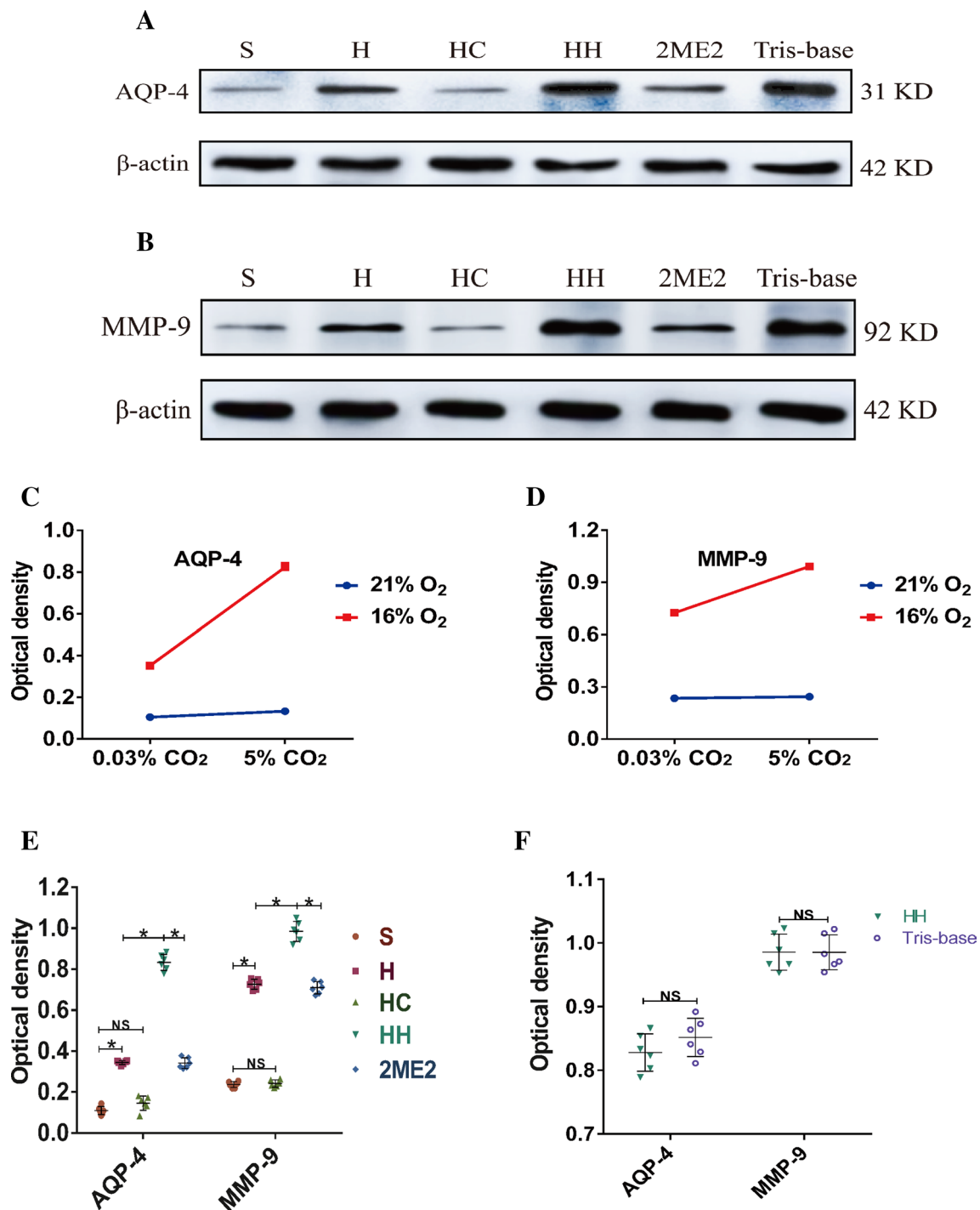
Fig. 5 The immunoreactive bands of total AQP-4 (**a**), MMP-9 (**b**), β-actin (**a**, **b**). β-actin expression was measured as control; There are significant interaction effects between hypercapnia treatment and hypoxia treatment (**c** AQP-4, *$p < 0.05$; **d** MMP-9, *$p < 0.05$). Effects of hypercapnia and 2ME2 on the protein expression levels of AQP-4 (**e**), MMP-9 (**e**) in each group (n = 6). Effects of Tris-base on the pro-tein expression levels of AQP-4 (**f**), MMP-9 (**f**) in each group (n = 6). The expression of AQP-4 and MMP-9 was normalized with β-actin protein level. Each data point refers to a biological replicate (n = 6). Horizontal lines (black) indicate mean ± SD (simple effects analyses). *$p < 0.05$; *NS* non-significant, $p > 0.05$. *MMP-9* matrix metallopro-teinase-9; *AQP-4* Aquaporins-4 (Color figure online)

$p = 0.005$, Fig. 7e; AQP-4: white arrow in Fig. 8a, Fluorescence density: df = 1, $F = 19.49$, $p = 0.004$, Fig. 8c and %AQP-4 positive cells: df = 1, $F = 27.75$, $p < 0.001$,

Fig. 8e; MMP-9: white arrow in Fig. 9a, Fluorescence density: df = 1, $F = 37.16$, $p < 0.001$, Fig. 9c and %MMP-9 positive cells: df = 1, $F = 50.19$, $p < 0.001$, Fig. 9e).
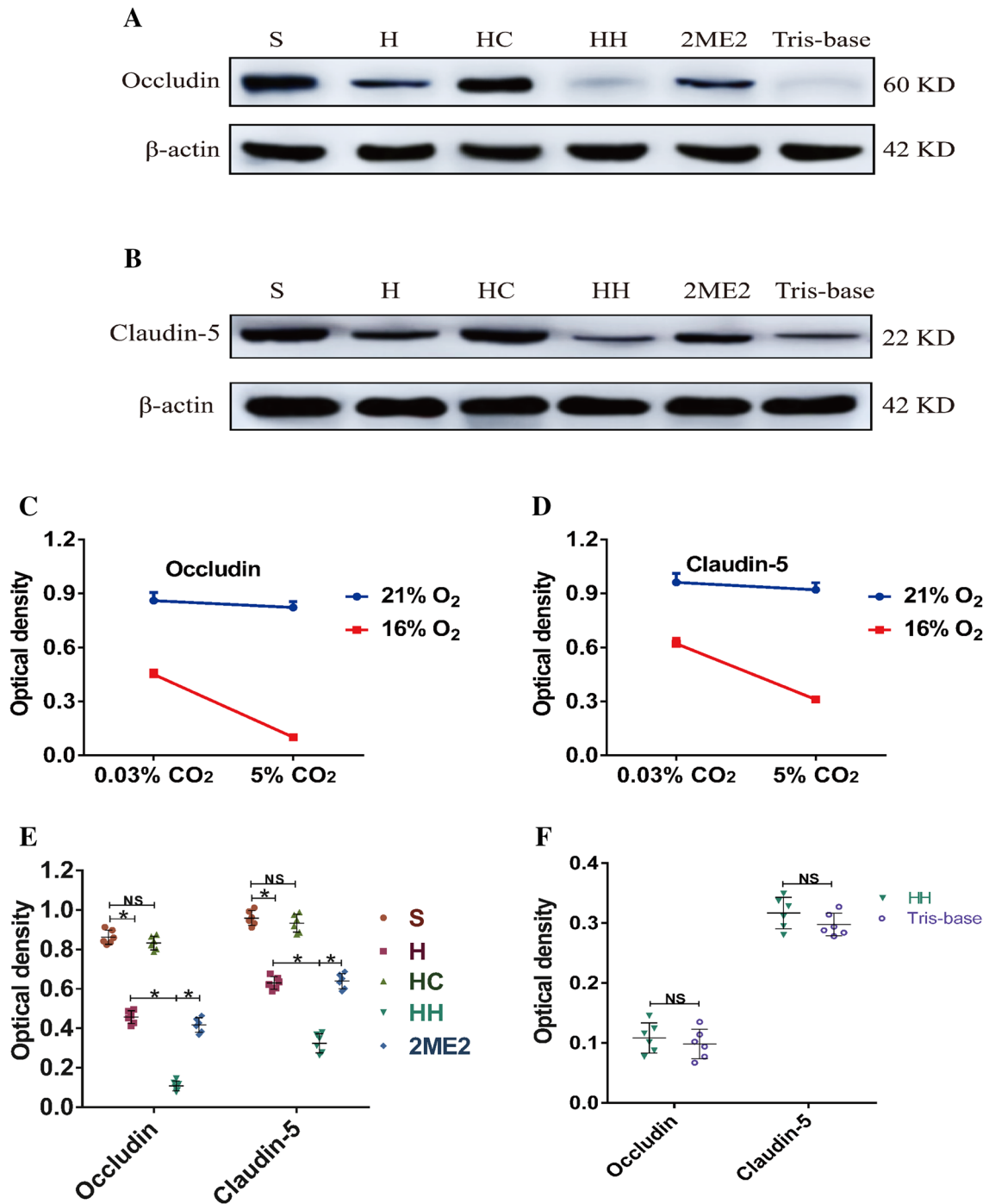
Fig. 6 The immunoreactive bands of total Occludin (**a**), Claudin-5 (**b**), β-actin (**a**, **b**). β-actin expression was measured as control; There are significant interaction effects between hypercapnia treatment and hypoxia treatment (**c** Occludin, *$p < 0.05$; **d** Claudin-5, *$p < 0.05$). Effects of hypercapnia and 2ME2 on the protein expression levels of Occludin (**e**), Claudin-5 (**e**) in each group (n=6). Effects of Tris-base on the protein expression levels of Occludin (**f**), Claudin-5 (**f**) in each group (n=6). The expression of Occludin, Claudin-5 was normalized with β-actin protein level. Each data point refers to a biological replicate (n=6). Horizontal lines (black) indicate mean±SD (simple effects analyses).*$p < 0.05$; *NS* non-significant, $p > 0.05$ (Color figure online)

Additionally, when the hypercapnic acidosis was neutralized, immunofluorescence of AQP-4, MMP-9 and nuclear HIF-1α between the HH group and the Tris-base group was comparable (nuclear HIF-1α: white arrow in Fig. 7b, Fluorescence density: $p = 0.858$, Fig. 7d and %HIF-1α positive cells: $p = 0.835$ in Fig. 7f; AQP-4: white arrow

Fig. 7 Confocal immunofluorescence images showing the expression of HIF-1α/GFAP/DAPI (white arrow) of the brain sections from the CA1 hippocampus in each group (**a**, **b** n=6). The average nuclear HIF-1α fluorescence (red) density of one single astrocyte in four fields of view per slice was analyzed in each group by the Image-Pro Plus software (**c**, **d**). The percentage of HIF-1α positive cells in four fields of view per slice was calculated in each group (**e**, **f**). Each data point refers to four fields of view per slice, where n=24 (4×6, biological replicates). Horizontal lines (black) indicate mean±SD. Statistical significance was examined by t test. *p < 0.05; NS non-significant, p > 0.05. HIF-1α hypoxia-inducible factor-1α. Scale bars: 50 μm (Color figure online)
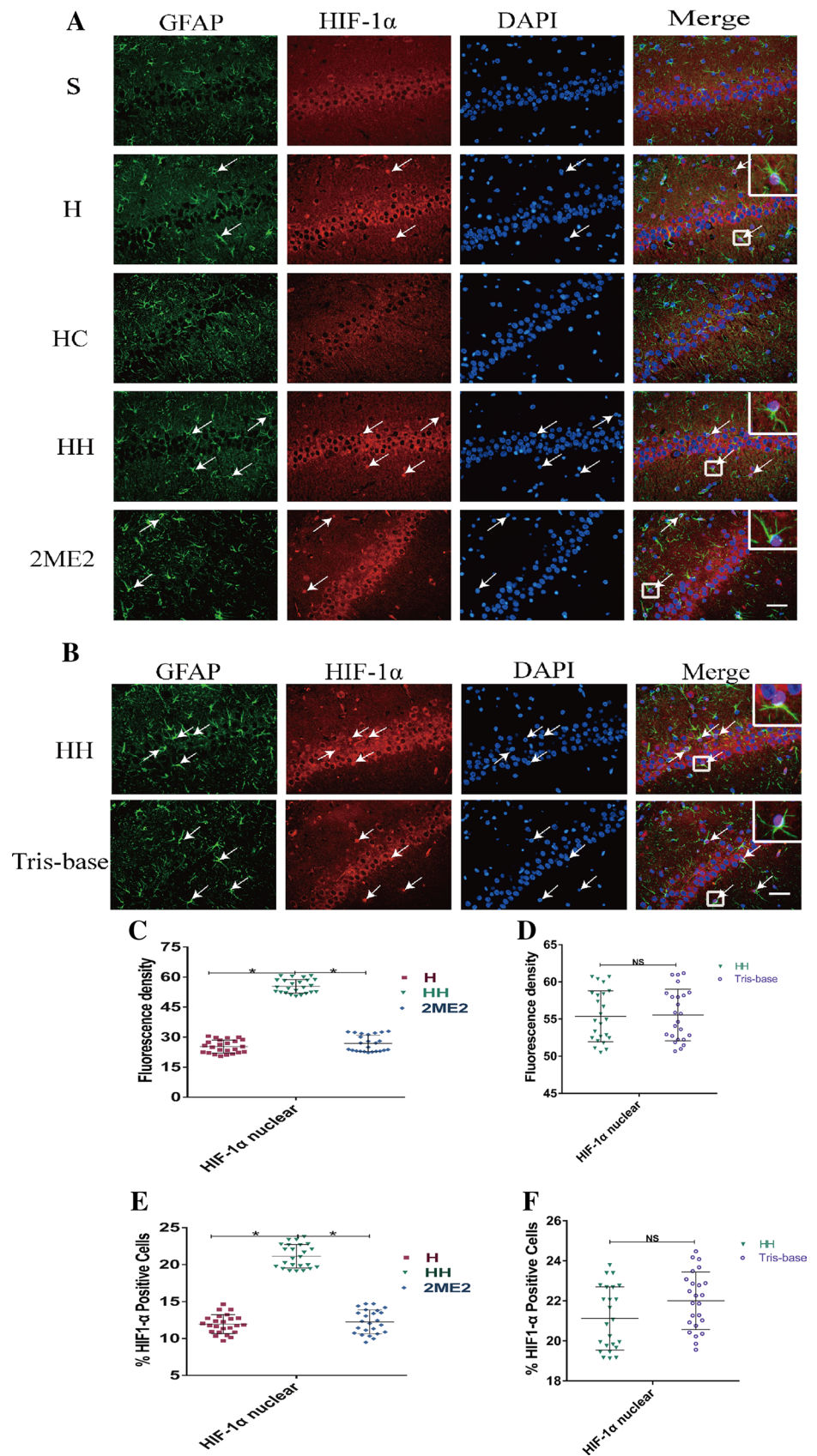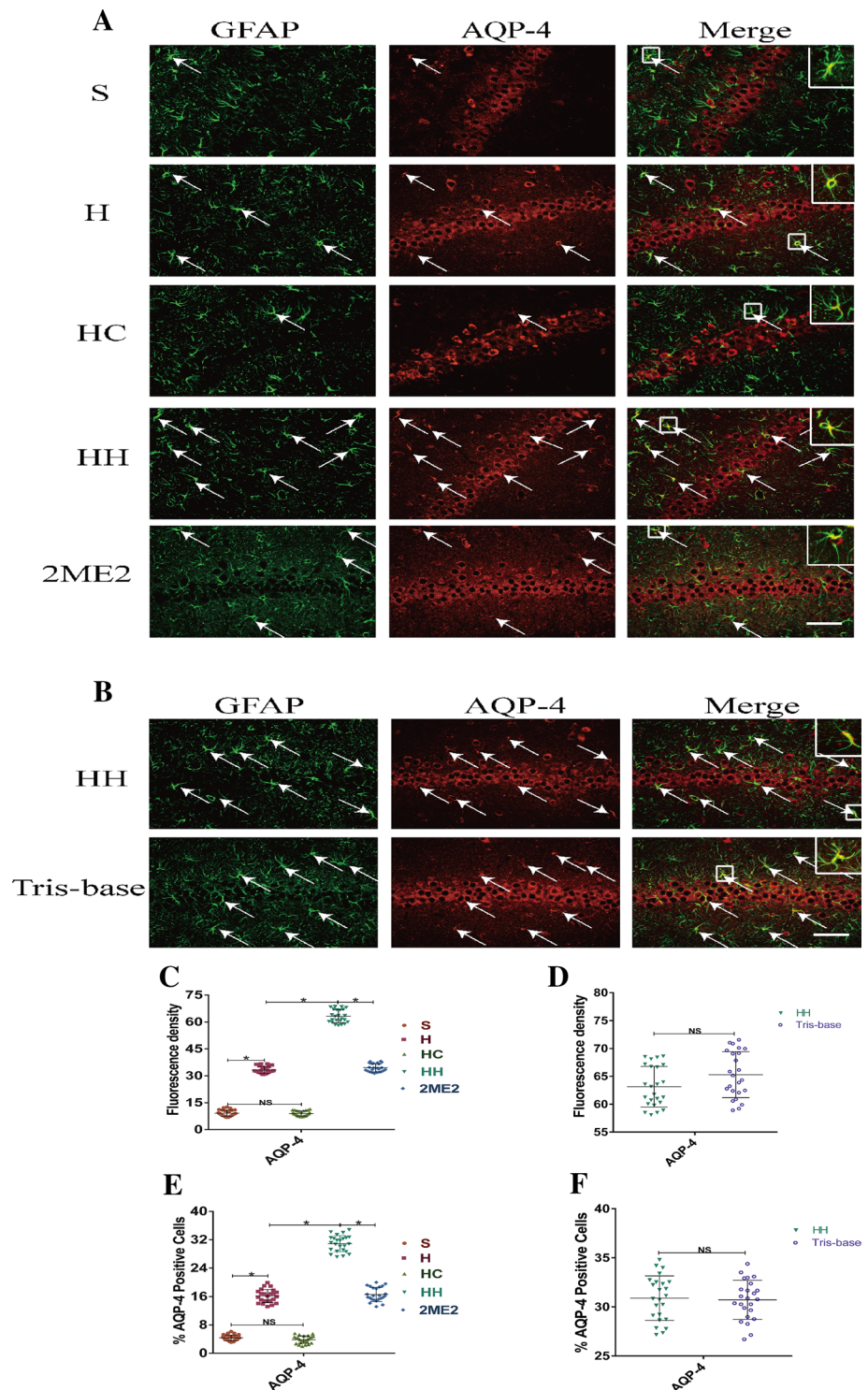
Fig. 8 Confocal immunofluorescence images showing the expression of AQP4/GFAP (white arrow) of the brain sections from the CA1 hippocampus in each group (**a**, **b**, n = 6). The average AQP4 fluorescence (red) density of one single astrocyte in four fields of view per slice was analyzed in each group by the Image-Pro Plus software (**c**, **d**). The percentage of AQP4 positive cells in four fields of view per slice was calculated in each group (E, F). Each data point refers to four fields of view per slice, where n = 24 (4 × 6, biological replicates). Horizontal lines (black) indicate mean ± SD. Statistical significance was examined by t test. *$p < 0.05$; *NS* non-significant, $p > 0.05$. *AQP-4* Aquaporins-4; Scale bars: 50 μm (Color figure online)


in Fig. 8b, Fluorescence density: $p = 0.779$, Fig. 8d and %AQP-4 positive cells: $p = 0.763$ in Fig. 8f; MMP-9: white arrow in Fig. 9b, Fluorescence density: $p = 0.839$, Fig. 9d and %MMP-9 positive cells: $p = 0.881$ in Fig. 9f). The individual data of the above each group were shown in the Supplemental Document. docx/Supplemental Table 5.

Discussion

The present results have shown that hypercapnia could further disrupt the integrity of BBB in the hypoxemic adult rats. Additionally, we have shown that hypercapnia

Fig. 9 Confocal immunofluorescence images showing the expression of MMP-9/GFAP (white arrow) of the brain sections from the CA1 hippocampus in each group (**a**, **b**, n = 6). The average MMP-9 fluorescence (red) density of one single astrocyte in four fields of view per slice was analyzed in each group by the Image-Pro Plus software (**c**, **d**). The percentage of MMP-9 positive cells in four fields of view per slice was calculated in each group (**e**, **f**). Each data point refers to four fields of view per slice, where n = 24 (4 × 6, biological replicates). Horizontal lines (black) indicate mean ± SD. Statistical significance was examined by t test. *$p < 0.05$; *NS* non-significant, $p > 0.05$. *MMP-9* matrix metalloproteinase-9; Scale bars: 50 μm (Color figure online)
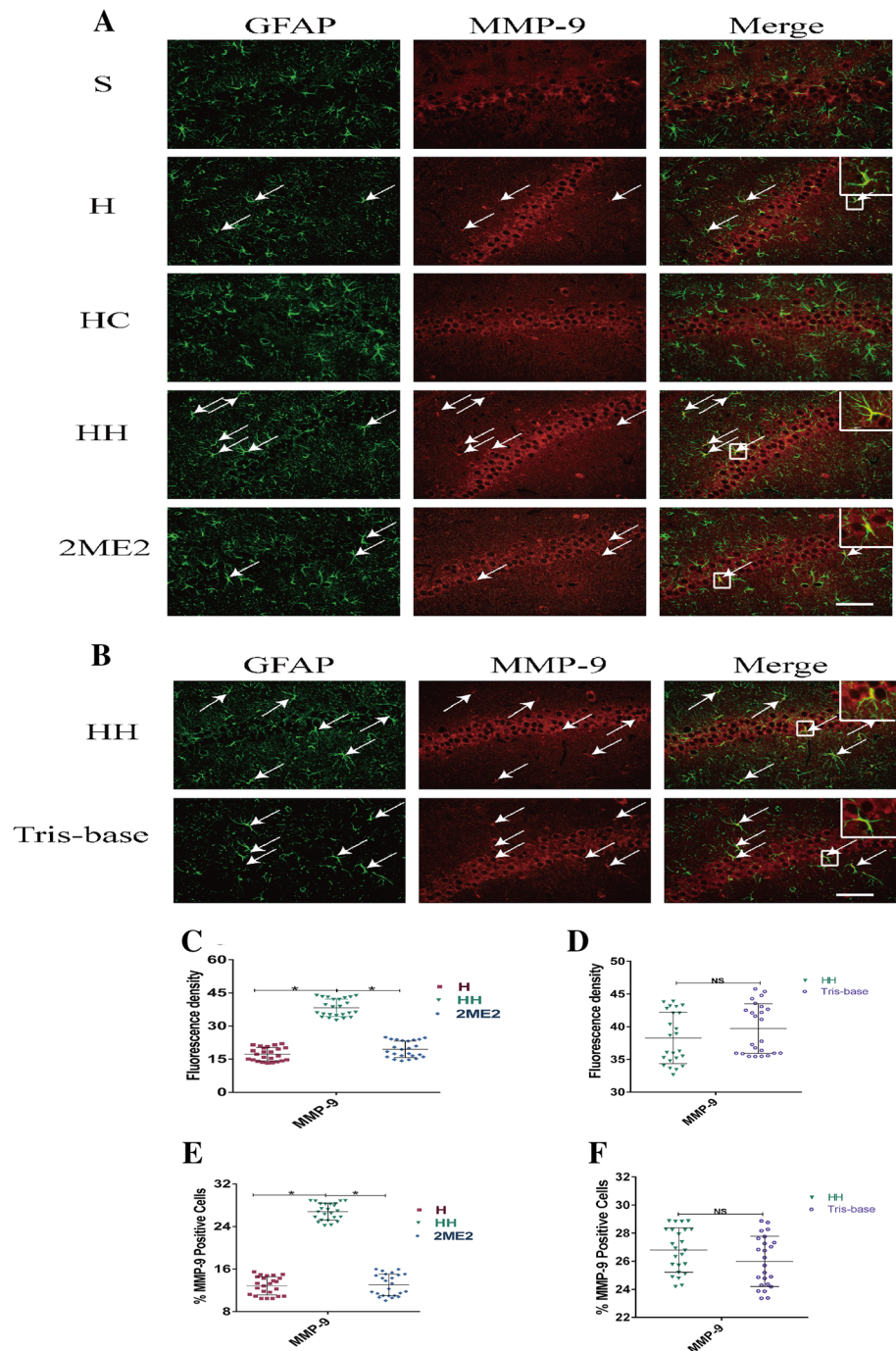
induces the HIF-1α nuclear translocation and over-expression of MMP-9 and AQP-4 proteins in hypoxia-activated astrocytes. It is suggested that this had contributed to further disruption of the BBB in the hypoxemic adult rats.

Previous studies indicated that hypercapnia can result in more severe cognitive dysfunction [6, 7]. In our present study, a rat model of hypercapnia/hypoxemia was established, in which PaO_2 was maintained at 55–60 mmHg and $PaCO_2$ was around 65 mmHg with a pH value at 7.20–7.25.

This is consistent with the clinical scenarios of COPD and ARDS. In agreement with our previous study [7], we confirmed here that hypercapnia alone did not sufficiently lead to cognitive dysfunction, but it significantly aggravated the cognitive dysfunction when applied in combination with hypoxemia. Of note, the effect exerted by hypercapnia is independent of the acidosis induced by itself. Furthermore, pretreatment with 2ME2 can prevent the exacerbation of cognitive impairment by hypercapnia.

Despite the above findings, the underlying molecular mechanisms exerted by hypercapnia have remained to be fully clarified. Previous studies have indicated that disruption of the BBB is closely related with the cognitive dysfunction [8, 9]. Furthermore, a recent study has reported that the BBB breakdown in the hippocampus may contribute to the cognitive impairment [12]. In the hypoxic-ischemic models of rats, the BBB integrity was impaired [34, 35]. Hence, we have shown that the BBB permeability was enhanced 3 h after hypoxemic insult in the hypoxemia group. More importantly, hypercapnia can further increase the BBB permeability in the hypercapnia + hypoxemia group. Very interestingly, when the acidosis was neutralized by the tris-base, the further enhanced BBB permeability could not be restored. Taken together, we speculate that hypercapnia may aggravate the cognitive dysfunction through further disruption of the BBB integrity in the hypoxemic hippocampus of rats independently of acidosis.

It is well documented that both the astrocytes and TJPs play important roles in maintaining the BBB integrity. First of all, with the AQP-4 protein in astrocytes being up-regulated, the BBB permeability was enhanced [36, 37]. Secondly, being the most important part of the TJPS, the decrease in the occludin and claudin-5 represents the enhanced permeability of the BBB [19, 20]. Under the hypoxic-ischemic conditions, occludin and claudin-5 can be degraded by MMP-9 released from the astrocytes in the brain [38, 39]. Furthermore, MMP-9 and AQP-4 can be regulated by the HIF-1 signaling pathway. Previous studies had demonstrated that the up-regulated expression of HIF-1α could induce the up-regulation of the MMP-9 and AQP-4 proteins which would eventually disrupt the BBB integrity [25, 26]. Consistent with this, we had found that 3 h after hypoxemic insult, the MMP-9 and AQP-4 protein expression was increased with a concomitant up-regulation of the total and nuclear HIF-1α protein in the H group. Additionally, we have found that hypercapnia alone did not affect the total and nuclear HIF-1α, MMP-9 and AQP-4 protein production in the astrocytes in the hippocampus. However, in comparison with the hypoxemia group, hypercapnia can induce an increase in nuclear HIF-1α, MMP-9 and AQP-4 protein production in hypercapnia + hypoxemia group. Following 2ME2 pretreatment, nuclear HIF-1α protein in the astrocytes was decreased in comparison with the hypercapnia + hypoxemia group.

In light of the above findings, it is suggested that 2ME2 can confer neuroprotection through improvement of the hypercapnia-indued exacerbation of the BBB disruption. It is documented that 2ME2 is a potent anticancer drug and that it is not a specific inhibitor for HIF-1a [29]. 2ME2 mainly exerts its physiological effects through vasodilatory, pro-apoptotic, tubulin-binding activity in cancer diseases and inhibition of HIF-1a nuclear translocation in non-cancer CNS diseases [40]. The vasodilatory effect of 2ME2 is poorly explored until recently. Previous studies have shown that 2ME2 inhibits phenylephrine-induced tension in the aorta [41] and KCl-induced contraction in the coronary artery [42] through its vasodilatory effect. However, the vasodilatory effect of 2ME2 in the brain have not been explored. The pro-apoptotic effect of 2ME2 is now well-recognized 2ME2 can induce cell death in a variety of malignant cell lines [43]. Tubulin-binding activity is also an important mechanism by which 2ME2 can inhibit tubulin polymerization and induce cell death in cancer cells [44]. However, 2ME2-mediated neuroprotection as reported in this study is unlikely to result from the pro-apoptotic and tubulin-binding activity, because 2ME2 did not induce apoptosis and inhibit tubulin polymerization in normal mammalian cells [45]. Taken together, it is suggested that 2ME2 can confer neuroprotection through inhibition of HIF-1a nuclear translocation in non-cancer CNS diseases.

In consideration of the above, it is suggested that hypercapnia can further increase the BBB permeability via facilitation of HIF-1α nuclear translocation in the astrocytes of hypoxemic rats. It is well known that hypercapnia is generally accompanied by acidosis in *vivo*. Therefore, cellular effects as observed under conditions of hypercapnic acidosis could be a consequence of elevated CO_2, decreased pH, or a combination of both [46]. To illustrate this, we next examined whether the pH levels would affect the nuclear translocation of HIF-1α protein. After neutralizing the acidosis induced by the hypercapnia through adding tris-base, we found that the effects mentioned above were not reversed. It stands to reason, therefore, that hypercapnia exerts its effect that is independent of the acidosis.

In conclusion, this study has demonstrated unequivocally that besides hypoxemia, hypercapnia also serves as an external stimulus that can trigger the intracellular signaling molecules which affect the expression of different proteins in the CNS. In this connection, hypercapnia can facilitate the nuclear translocation of HIF-1α protein, and then induce MMP-9 and AQP-4 protein over-expression in the astrocytes, which would further disrupt the BBB integrity in the hypoxemic rats. It is conceivable that further disruption of the BBB would partly ascribe to the etiopathogenesis of cognitive impairment. Thus, the cascade of hypercapnia-induced nuclear HIF-1α protein translocation in hypoxia-activated astrocytes may be a potential target for ameliorating cognitive impairment.

Compliance with Ethical Standards

Conflicts of interest The authors declare no conflict of interest.

References:s

1. Yang H, Xiang PC, Zhang EM et al (2015) Is hypercapnia associated with poor prognosis in chronic obstructive pulmonary disease? A long-term follow-up cohort study. BMJ Open 5:12

2. Laffey JG, O'Croinin DF, McLoughlin P et al (2004) Permissive hypercapnia: role in protective lung ventilatory strategies. Intensive Care Med 30:347–356

3. Schou L, Ostergaard B, Rasmussen LS et al (2012) Cognitive dysfunction in patients with chronic obstructive pulmonary disease systematic review. Respir Med 106(8):1071–1081

4. Mikkelsen ME, Christie JD, Lanken PN et al (2012) The adult respiratory distress syndrome cognitive outcomes study: long-term neuropsychological function in survivors of acute lung injury. Am J Respir Crit Care 185:1307–1315

5. Wolters AE, Slooter AJ, van der Kooi AW et al (2013) Cognitive impairment after intensive care unit admission: a systematic review. Intensive Care Med 39:376–386

6. Singh B, Mielke MM, Parsaik AK et al (2014) A prospective study of chronic obstructive pulmonary disease and risk of mild cognitive impairment. JAMA Neurol 71(5):581

7. Ding HG, Deng YY, Yang RQ et al (2018) Hypercapnia induces IL-1β overproduction via activation of NLRP3 inflammasome: implication in cognitive impairment in hypoxemic adult rats. J Neuroinflamm 15:4

8. Zlokovic BV (2008) The blood–brain barrier in health and chronic neurodegenerative disorders. Neuron 57(2):178–201

9. Wardlaw JM, Sandercock PA, Dennis MS et al (2003) Is breakdown of the blood-brain barrier responsible for lacunar stroke, leukoaraiosis, and dementia? Stroke 34(3):806–812

10. Stranahan AM, Hao S, Dey A (2016) Blood-brain barrier breakdown promotes macrophage infiltration and cognitive impairment in leptin receptor-deficient mice. J Cerebr Blood Flow Metab 36(12):2108–2121

11. Squire LR (1992) Memory and the hippocampus: a synthesis from findings with rats, monkeys, and humans. Psychol Rev 99(2):195–231

12. Montagne A, Barnes SR, Sweeney MD et al (2015) Blood-brain barrier breakdown in the aging human hippocampus. Neuron 85:296–302

13. Hawkins BT, Davis TP (2005) The blood–brain barrier/neurovascular unit in health and disease. Pharmacol Rev 57(2):173

14. Abbott NJ, Rönnbäck L, Hansson E (2006) Astrocyte-endothelial interactions at the blood-brain barrier. Nat Rev Neurosci 7(1):41–53

15. Zhao Z, Nelson AR, Betsholtz C et al (2015) Establishment and dysfunction of the blood-brain barrier. Cell 163(5):1064–1078

16. Francesca B, Rezzani R (2010) Aquaporin and blood brain barrier. Curr Neuro Pharmacol 8:92–99

17. Kaur C, Sivakumar V, Zhang Y (2006) Hypoxia-induced astrocytic reaction and increased vascular permeability in the rat cerebellum. Glia 54(8):826–839

18. YangWC ZhangXZ, Wang N et al (2016) Effects of acute systemic hypoxia and hypercapnia on brain damage in a rat model of hypoxia-ischemia. PLoS ONE 11(12):e0167359

19. Lochhead JJ, McCaffrey G, Quigley CE et al (2010) Oxidative stress increases blood-brain barrier permeability and induces alterations in occludin during hypoxia-reoxygenation. J Cerebr Blood Flow Metab 30:1625–1636

20. Jiao HX, Wang ZH, Liu YH et al (2011) Specific role of tight junction proteins claudin-5, occludin, and ZO-1 of the blood-brain barrier in a focal cerebral ischemic insult. J Mol Neurosci 44(2):130–139

21. Rempel RG, Hartz AM, Bauer BR (2016) Matrix metalloproteinases in the brain and blood–brain barrier: versatile breakers and makers. J Cerebr Blood Flow Metab 36(9):1481–1507

22. Borke WB, Munkeby BH, Halvorsen B et al (2004) Increased myocardial matrix metalloproteinases in hypoxic newborn pigs during resuscitation: effects of oxygen and carbon dioxide. Eur J Clin Invest 34:459–466

23. Wang GL, Jiang BH, Rue EA et al (1995) Hypoxia-inducible factor 1 is a basic-helix-loop-helix-PAS heterodimer regulated by cellular O_2 tension. Proc Natl Acad Sci USA 92:5510–5514

24. Sharp FR, Bernaudin M (2004) HIF1 and oxygen sensing in the brain. Nat Rev Neurosci 5:437–448

25. Higashida T, Ding YC, Kreipke C et al (2011) The role of hypoxia-inducible factor-1, aquaporin-4 and matrix metalloproteinase-9 in blood–brain barrier disruption and brain edema after traumatic brain injury. J Neurosurg 114(1):92

26. Wang Z, Meng CJ, Shen XM et al (2012) Potential contribution of hypoxia-inducible factor-1α, aquaporin-4, and matrix metalloproteinase-9 to blood–brain barrier disruption and brain edema after experimental subarachnoid hemorrhage. J Mol Neurosci 48:273–280

27. Budweiser S, Jörres RA, Feifer P et al (2008) Treatment of respiratory failure in COPD. Int J Chron Obstruct Pulmon Dis 3:605–618

28. Contreras M, Masterson C, Laffey JG (2015) Permissive hypercapnia: what to remember. Curr Opin Anaesthesiol 28:26–37

29. Orihuela PA, Rincion-Rodriguez R, Diaz P et al (2011) Role of 2-methoxyestradiol, an endogenous estrogen metabolite, in health and disease. Mini-Rev Med Chem 15(5):427–438

30. Peyrat JF, Brion JD, Alami M (2012) Synthetic 2-methoxyestradiol derivatives: structure-activity relationships. Curr Med Chem 19(24):4142–4156

31. Mueck AO, Seeger H (2010) 2-Methoxyestradiol-biology and mechanism of action. Steroids 75(10):625–631

32. Wu C, Hu Q, Chen JY et al (2013) Inhibiting HIF-1α by 2ME2 ameliorates early brain injury after experimental subarachnoid hemorrhage in rats. Biochem Biophys Res Commun 437(3):469–474

33. Asadbegin M, Yaghmaei P, Salehi I (2017) Investigation of thymol effect on learning and memory impairment induced by intrahippocampal injection of amyloid beta peptide in high fat diet-fed rats. Metab Brain Dis 32:827–839

34. Belayev L, Busto R, Zhao WZ (1996) Quantitative evaluation of blood-brain barrier permeability following middle cerebral artery occlusion in rats. Brain Res 739:88–96

35. DelZoppo GJ, Mabuchi T (2003) Cerebral microvessel responses to focal ischemia. J Cerebr Blood Flow Metab 23:879–894

36. Manley GT, Fujimura M, Ma TH et al (2000) Aquaporin-4 deletion in mice reduces brain edema after acute water intoxication and ischemic stroke. Nat Med 6:159–163

37. Papadopoulos MC, Verkman AS (2005) Aquaporin-4 gene disruption in mice reduces brain swelling and mortality in pneumococcal meningitis. J Biol Chem 280:13906–13912

38. Boroujerdi A, Welser-Alves JV, Milner R (2015) Matrix metalloproteinase-9 mediates post-hypoxic vascular pruning of cerebral blood vessels by degrading laminin and claudin-5. Angiogenesis 18(3):255–264

39. Bauer AT, Burgers HF et al (2010) Matrix metalloproteinase-9 mediates hypoxia-induced vascular leakage in the brain via tight junction rearrangement. J Cerebr Blood Flow Metab 30:837–848

40. Sathish Kumar B, Raghuvanshi DS, Hasanain M et al (2016) Recent Advances in chemistry and pharmacology of

2-methoxyestradiol: an anticancer investigational drug. Steroids 110:9–34

41. Hill BJ, Gebre S, Schlicker B et al (2010) Nongenomic inhibition of coronary constriction by 17ss-estradiol, 2-hydroxyestradiol, and 2-methoxyestradiol. Can J Physiol Pharmacol 88(2):147–152

42. Goyache FM, Gutierrez M, Hidalgo A et al (1995) Nongenomic effects of catechol estrogens in the in vitro rat uterine contraction. Gen Pharmacol 26(1):219–223

43. Hansen TV, Vik A, Akselsen OW et al (2015) Synthesis and pharmacological effects of the anti-cancer agent 2-methoxyestradiol. Curr Pharm Des 1(38):5453–5466

44. Kamath K, Okouneva T, Larson G et al (2006) 2-Methoxyestradiol suppresses microtubule dynamics and arrests mitosis without depolymerizing microtubules. Mol Cancer Ther 5(9):2225–2233

45. Huang P, Feng L, Oldham EA, Keating MJ et al (2000) Superoxide dismutase as a target for the selective killing of cancer cells. Nature 407:390–395

46. Cummins EP, Selfridge AC, Sporn PH et al (2014) Carbon dioxide-sensing in organisms and its implications for human disease. Cell Mol Life Sci 71:831–845